

A Novel Optimal Fuzzy System for Color Image Enhancement Using Bacterial Foraging

Madasu Hanmandlu, *Senior Member, IEEE*, Om Prakash Verma, Nukala Krishna Kumar, and Muralidhar Kulkarni

Abstract—A new approach is presented for the enhancement of color images using the fuzzy logic technique. An objective measure called exposure has been defined to provide an estimate of the underexposed and overexposed regions in the image. This measure serves as the dividing line between the underexposed and overexposed regions of the image. The hue, saturation, and intensity (HSV) color space is employed for the process of enhancement, where the hue component is preserved to keep the original color composition intact. A parametric sigmoid function is used for the enhancement of the luminance component of the underexposed image. A power-law operator is used to improve the overexposed region of the image, and the saturation component of HSV is changed through another power-law operator to recover the lost information in the overexposed region. Objective measures like fuzzy contrast and contrast and visual factors are defined to make the operators adaptive to the image characteristics. Entropy and the visual factors are involved in the objective function, which is optimized using the bacterial foraging algorithm to learn the parameters. Gaussian and triangular membership functions (MFs) are chosen for the underexposed and overexposed regions of the image, respectively. Separate MFs and operators for the two regions make the approach universal to all types of contrast degradations. This approach is applicable to a degraded image of mixed type. On comparison, this approach is found to be better than the genetic algorithm (GA)-based and entropy-based approaches.

Index Terms—Contrast factor, entropy, exposure, fuzzifier, image enhancement, intensification, overexposed image, underexposed image, visual factor.

I. INTRODUCTION

ONE of the most common defects found in a recorded image is its poor contrast. This degradation may be caused by inadequate lighting, the aperture size, the shutter speed, and the nonlinear mapping of the image intensity. The effect of such defects is reflected on the range and shape of the gray-level histogram of the recorded image. Image enhancement

Manuscript received December 22, 2007; revised June 9, 2008. First published May 2, 2009; current version published July 17, 2009. The Associate Editor coordinating the review process for this paper was Dr. Cesare Alippi.

M. Hanmandlu is with the Department of Electrical Engineering, Indian Institute of Technology, New Delhi 110016, India (e-mail: mhmandlu@ee.iitd.ac.in).

O. P. Verma is with the Department of Information and Technology, Delhi College of Engineering, New Delhi 110042, India (e-mail: opverma.dce@gmail.com).

N. K. Kumar is with the Motorola India Pvt. Ltd., Hyderabad 500081, India (e-mail: krishna.dce@gmail.com).

M. Kulkarni is with the Department of Electronics and Communication Engineering, National Institute of Technology Karnataka, Surathkal 575025, India (e-mail: mkuldcce@gmail.com).

Color versions of one or more of the figures in this paper are available online at <http://ieeexplore.ieee.org>.

Digital Object Identifier 10.1109/TIM.2009.2016371

techniques achieve improvement in the quality of the original image or provide additional information that was not apparent in the original image. It improves the appearance of an image by increasing the dominance of some features or by decreasing the ambiguity between different regions of the image.

Several image enhancement algorithms exist in the spatial domain. One of these kinds is reported in [1], where the image enhancement based on the human perception (retinex) achieves color constancy and dynamic range compression. Velde [2] attempts to enhance the color image in the LUV color space, where each component is used to find the gradients, and these gradients (differences) are enhanced using the conventional gray-level enhancement techniques like contrast stretching. Tao and Asari [3] extend the approach in [1], where the color saturation adjustment for producing more natural colors is implemented. However, these techniques fail to enhance all the images, as they do not preserve the original colors in the enhanced image.

Eschbach and Webster [4] propose a method for altering the exposure in an image, by iteratively comparing the intensity with a pair of preset thresholds T_{light} and T_{dark} , which indicate the satisfactory brightness and darkness, respectively, while processing the image until the threshold conditions are satisfied. Eschbach and Kolpatzik [5] also suggest a method for correcting the color saturation in natural scene images, by iteratively processing and comparing the average saturation with the preset threshold T_{sat} .

Image enhancement approaches may introduce color artifacts if directly applied to the three components [red, green, and blue (RGB)] of a degraded color image. Therefore, direct enhancement of the RGB color space is inappropriate for the human visual system. A proper color space should decouple the chromatic information from the achromatic information. Hue, saturation, and intensity (HSV) values are the three components of one such color space. In the spectrum, each color is at the maximum purity (or strength or richness) that the eye can perceive, and the spectrum of colors is diluted by mixing with other colors or with white light; its richness or saturation is decreased thereafter.

In the process of color image enhancement, the original color (hue) of the image should not be disturbed, and the values of other components should not exceed the maximum value of the image. Hue-preserved color image enhancement is presented in [6], and this generalizes the existing gray-scale contrast intensification techniques to color images. Here, a principle is suggested to make the transformations “gamut problem” free. However, these methods are not robust, as each approach is geared to a particular degraded image.

Shyu and Leoua [7] present a better approach based on genetic algorithms (GAs) for the color image enhancement, where a weighted combination of four types of nonlinear transforms (*s*-curves) is used as a transformation function. The weighting coefficients are calculated by optimizing an objective function, which is formed from the objective measures of the image such as Brenner's measure, and some noise information. However, this approach does not account for the ambiguities in the image.

Image processing has to deal with many ambiguous situations. Fuzzy set theory is a useful mathematical tool for handling the ambiguity or uncertainty. Therefore, fuzzy logic has come in a big way into the image processing area; the works of Pal and Rosenfeld [8] and Russo and Ramponi [9] are only the tip of the iceberg. The gray-level maximum does not change in the classical fuzzy enhancement method [8]; hence, it is of no use for degraded images with less dynamic range and low contrast. To surmount this problem, a generalized iterative fuzzy enhancement algorithm is proposed by Dong-liang and An-ke [10].

In the field of image enhancement and smoothing using the fuzzy framework, two contributions merit an elaboration. The first one frames "IF...THEN...ELSE" fuzzy rules [9] for image enhancement. Here, a set of neighborhood pixels constitutes the antecedent and the consequent clauses that serve as the fuzzy rule for the pixel to be enhanced. These fuzzy rules offer directives much similar to humanlike reasoning. The second one relates to a rule-based smoothing [11] in which different filter classes are devised on the basis of compatibility with the neighborhood. Russo [12] discusses the recent advances in fuzzy image processing. The *s*-curve is used in [13] as the transformation function, and its parameters (*a*, *b*, and *c*) are calculated by optimizing the entropy. These parameters select the shape and range of the transformation operator. The above approaches apply the operators to the luminance part of the color image, and they sometimes overenhance or underenhance the image because they do not account for the shape and range of the original histogram.

Hanmandlu *et al.* [14] propose a new intensification operator, i.e., NINT, which is a parametric sigmoid function for the modification of the Gaussian type of membership based on the optimization of entropy with respect to the parameters involved in the intensification operator. The approach in [15] describes an efficient enhancement using the fuzzy relaxation technique. Different orders of fuzzy membership functions (MFs) and different statistics are attempted to improve the enhancement speed and quality, respectively. These works have been confined to the enhancement of gray images only.

In the context of image processing, only a few papers address the issue of underexposed and overexposed images. Hanmandlu and Jha [16] use a global contrast intensification (GINT) operator, which is an extended NINT operator for the enhancement of the luminance part in the fuzzy domain, and also propose the quality factors. The parameters of this operator are found by optimizing the image entropy. This approach works well for underexposed images but fails for overexposed images and mixed exposed images.

Wang *et al.* [17] introduce a high-dynamic-range (HDR) image hallucination for accruing HDR details to the overexposed

and underexposed regions of a low-dynamic-range image. This technique though resolves the underexposed/overexposed issue but is not automatic, i.e., it needs the user's discretion to identify which patch needs to be pasted to the degraded region. It only tackles the issue of permanently degraded regions (described in Section III) and ignores the gray-level or saturation enhancement of other regions.

In this paper, we extend the approach in [16] for automatic enhancement of all types of degraded color images. The saturation component is also made variable along with the luminance (intensity), while keeping the hue of the image fixed to enhance the color image. An objective measure called exposure is devised to provide an amount of exposure of the image to light by considering the shape of the histogram of the intensity component of the image. Based on this measure, the image can be divided into underexposed and overexposed regions, and these can separately be modified by both GINT and power-law transformation operators. The parameters of the operators are adjusted to make them applicable to a particular type of degradation in the image. For the calculation of the parameters, an objective function is constructed by involving the entropy and the contrast and visual factors of the image. The minimization of this objective function leads to the enhancement of an image by stretching the intensity (*V*) component of the pixels about the crossover point.

The organization of the paper is given as follows. Section II introduces the image classification based on intensity exposition. Section III presents the fuzzification and intensification of luminance of the color image and the enhancement of saturation. In Section IV, we define the contrast and visual factors that help achieve the desired enhancement. The parameters of the GINT and power-law operators are determined by the optimization of the entropy using the bacterial foraging (BF) algorithm. The results are discussed in Section V, and conclusions are drawn in Section VI.

II. IMAGE CLASSIFICATION BASED ON INTENSITY EXPOSITION

Many images do not appear in the natural form because of poor contrast, as reflected by their histograms that do not occupy the whole dynamic range. The underlying intensity exposition may occupy more of the lower part or the upper part of the total range. When the gray levels contain more of the lower part of the histogram area, the region appears dark, whereas it appears very bright when its gray levels occupy more of the upper area of the histogram. Underexposed or overexposed regions in the image are a group of neighborhood pixels whose gray values are close to either the least or the highest of the available dynamic range, and the differences among their gray values are very low. In both cases, one cannot readily perceive the details in the image. There are certain images, called mixed exposed images, that contain both underexposed and overexposed regions in the same image. It may be noted that when dealing with the color images, only the *V* component of HSV, which is represented in gray levels, is utilized for the purpose of delineation of an image into underexposed and overexposed regions.

In reality, it may be observed that most of the images are of mixed type. It is rare to have truly underexposed or overexposed images. Therefore, a parameter called “exposure” is introduced to denote what percentage of the image gray levels is underexposed or overexposed. Hence, every image is now considered as a mixed image containing a certain percentage of each type of region. The parameter “exposure” denoting an amount of intensity exposition is given by

$$\text{exposure} = \frac{1}{L} \frac{\sum_{x=1}^L p(x) \cdot x}{\sum_{x=1}^L p(x)} \quad (1)$$

where x indicates the gray-level values of the image, $p(x)$ represents the histogram of the whole image, and L represents the total number of gray levels.

Although a single parameter cannot characterize both the underexposed and overexposed regions of the image, it provides information for applying a proper operator to automatically enhance both regions. This parameter is normalized in the range $[0, 1]$. If the value of exposure for a certain image is found to be more than 0.5, it implies that there is more overexposed region than underexposed region. It has been found that for a pleasing image, the exposure should be close to 0.5. Before the start of the enhancement process, every image is treated to be a mixed-type image, and then, an attempt is made to segment the image into underexposed and overexposed regions so that both regions can be processed separately.

Different operators are defined for enhancing the underexposed and overexposed images. Note that no image is solely underexposed or overexposed. For a mixed exposed image, both of these operators should simultaneously be applied to obtain a pleasing image. This can be achieved by first dividing the image gray levels into two parts. A new factor denoted by a in the range $[0, L - 1]$, divides the gray levels into two parts: $[0, a - 1]$ for underexposed images and $[a, L - 1]$ for overexposed images

$$a = L \cdot (1 - \text{exposure}). \quad (2)$$

III. FUZZIFICATION, INTENSIFICATION, AND ENHANCEMENT

In this paper, the HSV color model [18] is adopted for the purpose of enhancement. An important property of the HSV color model is that it separates the chromatic information from the achromatic information. To enhance the color image, the original color (hue) should be preserved. Here, the gray-level component (V) and the saturation component (S) are separately processed.

In many image processing applications, the image information to be processed is uncertain and ambiguous. For example, the question of whether a pixel should be turned darker or brighter from its original gray level comes under the realm of the fuzzy approach. In image processing, some objective quality criteria are usually defined to ascertain the goodness of the results, e.g., the image is good if it possesses a low amount of fuzziness indicating high contrast. The human observer,

however, does not perceive these results as good because his/her judgment is subjective and different people differently judge the image quality. Fuzzy techniques offer powerful tools that efficiently deal with the vagueness and ambiguity of images by associating a degree of belongingness to a particular property. Generally, fuzzy image processing has three main stages: image fuzzification, modification of membership values, and defuzzification. The choice of fuzzification function, contrast operators, and defuzzification function differ depending upon a particular application.

An image of size $M \times N$ having intensity levels x_{mn} in the range $[0, L - 1]$ can be considered as a collection of fuzzy singletons in the fuzzy set notation

$$I = \bigcup \{\mu(x_{mn})\} = \{\mu_{mn}/x_{mn}\}, \quad (3)$$

$$m = 1, 2, \dots, M; \quad n = 1, 2, \dots, N$$

where $\mu(x_{mn})$ or μ_{mn}/x_{mn} represents the membership or grade of some property μ_{mn} of x_{mn} , with x_{mn} being the color intensity at the (m, n) th pixel. For a color image, the MFs are computed only for the luminance component $X \in \{V\}$. To realize the computational efficiency, the histogram of X is considered for fuzzification instead of taking the intensity level at each pixel.

An image can be split up into underexposed and overexposed regions by using the value a . A modified Gaussian MF defined in [16] is used to fuzzify the underexposed region of the image as follows:

$$\mu_{X_u}(x) = \exp \left\{ - \left[\frac{x_{\max} - (x_{\text{avg}} - x)}{\sqrt{2}f_h} \right]^2 \right\} \quad (4)$$

where x indicates the gray level of the underexposed region in the range $[0, a - 1]$, x_{\max} is the maximum intensity level in the image, and x_{avg} is the average gray level value in the image. f_h is called a fuzzifier, and its initial value is found from

$$f_h^2 = \frac{1}{2} \frac{\sum_{x=0}^{L-1} (x_{\max} - x)^4 p(x)}{\sum_{x=0}^{L-1} (x_{\max} - x)^2 p(x)}. \quad (5)$$

A triangular MF is derived for the fuzzification of an overexposed region of the image for $x \geq a$ and is given by

$$\mu_{X_o}(x) = \begin{cases} 0 & x < a \\ \frac{x-a}{L-a} & x \geq a. \end{cases} \quad (6)$$

MFs transform the image intensity levels from the spatial domain into the fuzzy domain, where they have values in the range $[0, 1]$. The MFs defined above affect only the respective regions and do not alter the other regions. This is because the function of the sigmoid operator employing Gaussian MFs and that of the power-law operator of the triangular MFs are mutually exclusive. Gaussian MFs become operational below the exposure factor, whereas the triangular MFs become operational above this factor. The distribution of gray levels in the underexposed region is similar to Gaussian. Power law is a

kind of nonlinearity that helps reduce the high intensity values in the overexposed region. Moreover, to make the final intensity follow a power law, a linear MF such as a triangular MF must be selected. Hence, we have different forms for the MFs in the two operators to match the characteristics of the respective region.

The modified membership values of these two regions are converted back to the spatial domain, i.e., defuzzified, using the respective inverse MFs.

A parametric sigmoid function in [16] (or simply a *sigmoid operator*) for enhancing the MF values of the original gray levels of the underexposed region is given by

$$\mu'_{Xu}(x) = \frac{1}{1 + e^{-t(\mu_{Xu}(x) - \mu_c)}} \quad (7)$$

where t is the intensification parameter (or *intensifier*), and μ_c is the crossover point. A power-law transformation operator (or simply a *power-law operator*) is defined for the improvement of the overexposed region of the image. This is meant to improve the information of the original gray levels by modifying their MFs in this region. For an overexposed image, the gray levels of the image are stacked near the maximum gray level. The cumulative of the differences among the gray levels of neighboring pixels may be thought of as information content. Before applying the operator, differences among the neighborhood gray levels (i.e., information content) are very low. The function of the power-law operator is therefore to improve this information content by way of a power γ on the sum of the triangular MF for the exposed region plus a small value ε in the general case as follows:

$$\mu'_{Xo}(x) = K (\mu_{Xo}(x) + \varepsilon)^\gamma. \quad (8)$$

Here, we take $K = 1$ and $\varepsilon = 0$ for simplicity. In any image, the maximum gray level value is L or one (if normalized), and the pixel containing the maximum gray level appears white.

Note that with these operators, the information cannot be increased if all the gray levels of the overexposed region are at the maximum intensity value or all the gray levels of the underexposed region are at the minimum intensity value, i.e., zero. The part of the image area where all pixels are at the maximum/minimum intensity level is called the “permanently degraded region” of the image. As there is no information, improvement cannot be achieved by simply operating on the intensity values. This problem can partially be solved by changing the saturation, which may result in the restoration of information. The improvement in the “Rose” image can be noticed in Fig. 9. The method introduced in [17] can alternatively be used for achieving enhancement of the permanently degraded region in an image, by replenishing the information from a patch of the similar texture identified by the user.

It is observed that saturation plays a very important role for the enhancement of overexposed color images. As the value of saturation is reduced, images regain their details, thus attaining the pleasing nature. It may be noted here that the enhancement of saturation for all types of images is not trivial, as it sometimes overenhances the colors.

We should not blindly vary the saturation but instead judge how much the saturation of a particular image has to be changed

to avoid overenhancement. As per our observation, the underexposed images that have exposure values less than 0.5 need only a gradual amount of saturation enhancement. The saturation is needed only for certain degraded images and the amount of variation should depend on the portion of the overexposed or underexposed region in the image. Another power-law operator for the enhancement of saturation termed as the *saturation operator* is defined by

$$S'(x) = [S(x)]^{(1-0.5^* \text{exposure})} \quad (9)$$

where $S(x)$ and $S'(x)$ are the original and the modified saturation values of the HSV color space, respectively.

It is found that saturation may not be zero even when the intensity information is zero in the case of permanently degraded images. Modification of saturation restores the pleasing nature for such images.

IV. FUZZY MEASURES AND OPTIMIZATION

A. Fuzzy Contrast Measures

In this approach, a set of fuzzy contrast measures like contrast and visual factors are defined for the calculation of the final objective function. To make the proposed approach converge faster, appropriate performance measures must be chosen. Since image quality perception and evaluation are subjective and the human visual system is very complicated, it is not easy to find a suitable performance measure that can exactly respond to the actual image quality and match the characteristics of the human visual system. The fuzzy performance measures to be employed in this approach will approximate the actual image quality. The quality of the enhanced color images can be measured in two ways: 1) an objective and quantitative analysis of color image quality and 2) a subjective visual inspection of the images. The defined entropy and visual factors can be used as the quantitative measure of color image quality.

The fuzzy contrasts for an image are computed by calculating the deviation of the membership values from the crossover point. Two fuzzy contrasts are separately defined for both the underexposed and the overexposed regions.

The fuzzy contrast for the underexposed region of the image is given by

$$C_{fu} = \frac{1}{a} \cdot \sum_{x=0}^{a-1} (\mu'_{Xu}(x))^2. \quad (10)$$

The average fuzzy contrast for the underexposed region of image is

$$C_{afu} = \frac{1}{a} \cdot \sum_{x=0}^{a-1} (\mu'_{Xu}(x)). \quad (11)$$

The fuzzy contrast for the overexposed region of image is

$$C_{fo} = \frac{1}{L-a} \cdot \sum_{x=a}^{L-1} (1 - \mu'_{Xo}(x))^2. \quad (12)$$

The average fuzzy contrast for the overexposed region of image is

$$C_{af_o} = \frac{1}{L-a} \cdot \sum_{x=a}^{L-1} (1 - \mu'_{X_o}(x)). \quad (13)$$

The fuzzy contrast and the average fuzzy contrast for both the underexposed and overexposed regions of the original (starting symbolized by s) image are as follows:

$$C_{f_{us}} = \frac{1}{a} \cdot \sum_{x=0}^{a-1} (\mu_{X_u}(x))^2 \quad (14)$$

$$C_{af_{us}} = \frac{1}{a} \cdot \sum_{x=0}^{a-1} (\mu_{X_u}(x)) \quad (15)$$

$$C_{f_{os}} = \frac{1}{L-a} \cdot \sum_{x=a}^{L-1} (1 - \mu_{X_o}(x))^2 \quad (16)$$

$$C_{af_{os}} = \frac{1}{L-a} \cdot \sum_{x=a}^{L-1} (1 - \mu_{X_o}(x)). \quad (17)$$

In the above definition, the average fuzzy contrast gives the overall intensity of the image, whereas the fuzzy contrast gives the spread of the gradient with respect to the reference (the crossover point). Their ratio, called the contrast factor, is used to define the visual factor.

Definition: The contrast factor of an image is defined as the ratio of the absolute average fuzzy contrast to the fuzzy contrast. The contrast factor for the underexposed region of the modified image is

$$Q_{f_u} = |C_{af_u}/C_{f_u}|. \quad (18)$$

The respective contrast factor for the overexposed region of the modified image is

$$Q_{f_o} = |C_{af_o}/C_{f_o}|. \quad (19)$$

The definitions in (18) and (19) pertaining to the contrast factors provide a measure of the uncertainty. The MF depicts the uncertainty in the intensity values. The mean gives the average value of the uncertainty, and the square of this function gives the spread. Their ratio, i.e., average/spread, should give a measure that is characteristic of an image. It gives an idea about the amount of uncertainty in any image belonging to either the original image or the modified/enhanced image.

In view of the above definition, the contrast factor of the original image for the underexposed region is

$$Q_{f_{us}} = |C_{af_{us}}/C_{f_{us}}|. \quad (20)$$

The corresponding contrast factor for the overexposed region of the original image is

$$Q_{f_{os}} = |C_{af_{os}}/C_{f_{os}}|. \quad (21)$$

B. Definition of Entropy

Entropy that makes use of Shannon's function is regarded as a measure of quality of information in an image in the

fuzzy domain. It gives the value of indefiniteness of an image defined by

$$E = \frac{-1}{L \ln 2} \left[\sum_{x=0}^{a-1} \left[\mu'_{X_u}(x) \ln(\mu'_{X_u}(x)) + (1 - \mu'_{X_u}(x)) \ln(1 - \mu'_{X_u}(x)) \right] + \sum_{x=a}^{L-1} \left[\mu'_{X_o}(x) \ln(\mu'_{X_o}(x)) + (1 - \mu'_{X_o}(x)) \ln(1 - \mu'_{X_o}(x)) \right] \right]. \quad (22)$$

Since it provides useful information about the extent to which the information can be retrieved from the image, optimization of this should pave the way for the determination of the parameters: t , μ_c , f_h , and γ .

C. Visual Factors

For the purpose of judging the contrast factor, the normalized contrast factor, called the visual factor, is now defined. It specifies the amount of enhancement caused. Separate visual factors will be needed for the underexposed and the overexposed regions, and these can be combined using the exposure parameter. The visual factor for the underexposed region of the image is defined as

$$V_{f_u} = \frac{Q_{f_u}}{Q_{f_{us}}}. \quad (23)$$

The visual factor defined for the overexposed region of the image is

$$V_{f_o} = \frac{Q_{f_{os}}}{Q_{f_o}}. \quad (24)$$

The definitions in (23) and (24) pertaining to visual factors give another measure concerning the relative change in the image with respect to the original image after modification/enhancement. This is termed as a visual factor that gives an idea of a change in visual appearance. In this paper, this factor has been used to ascertain the visual assessment of both underexposed and overexposed regions.

Note that for the overexposed region, the original contrast factor $Q_{f_{os}}$ will be higher than the contrast factor Q_{f_o} . The visual factors have values greater than one for all images, and they need to be combined based on the amount of the underexposed and overexposed regions contained in the original image to yield an overall visual factor defined as

$$V_f = V_{f_u} \cdot (\text{exposure}) + V_{f_o} (1 - \text{exposure}). \quad (25)$$

The definition of the visual factor allows us to specify a range for the desired normalized contrast factor, and increasing its value beyond the range causes loss of the pleasing nature of the image. By experimentation, the visual factor is found to be in between 1.0 and 1.5 for a pleasing image.

D. Objective Function for Optimization

Since the entropy function is constructed from the MFs, it represents the uncertainty associated with the image information, and the difference in the visual factors also provides another measure of uncertainty associated with the change in the image information as a result of enhancement. Both measures contribute to the visual quality of the image; hence, these must be optimized. Therefore, if the desired visual factor V_{df} is known corresponding to V_f , then the attainment of their equality is posed as a constraint in the optimization of the entropy function. This process is the constrained optimization framed as [19]

Optimize the entropy function E
subject to the constraint $V_{df} = V_f$.

For this, an objective function is set up as under

$$J = E + \lambda |V_{df} - V_f|. \quad (26)$$

By giving equal weights to the two components on the right-hand side of (26), the need for Lagrangian multiplier λ is eliminated as different values of this multiplier are not found to have a bearing on the parameters. The optimization of the objective function is done by taking the parameters in the ranges $t \geq 1$, $0 \leq \mu_c \leq 1$, and $\gamma \geq 1$. For this purpose, the modified BF optimization algorithm, which assures quick convergence, is employed. A brief description of the BF is relegated to Appendix A.

E. Modified BF

The BF algorithm in [20], described in Appendix A, is modified to expedite the convergence. The modifications made are: 1) instead of the average value, the minimum value of all the chemotactic cost functions is retained for deciding the bacterium's health to speed up the convergence, and 2) to reduce the complexity, the cell-to-cell attractant function is ignored in swarming.

The selection of the initial parameters of the algorithm, such as the number of iterations and the final error value, plays a key role in deciding the accurate optimum values in lesser time. These parameters are not constant for all applications but rather depend on the application. The flowchart of the modified BF optimization algorithm is shown in Fig. 1.

F. Initialization of Parameters

This includes two sets of parameters: the parameters (n_p) to be optimized, i.e., t , μ_c , f_h , and γ in the original objective function J , and the parameters of the BF entering into J to make it a time-varying cost function for facilitating the optimization. The initialization of the former will be given in the enhancement algorithm later, and the initialization of the latter is now taken up.

- 1) The number of bacteria $N_b = 12$.
- 2) The swimming length $N_s = 4$.
- 3) The number of iterations in a chemotactic loop N_c is set to 25 ($N_c > N_s$).

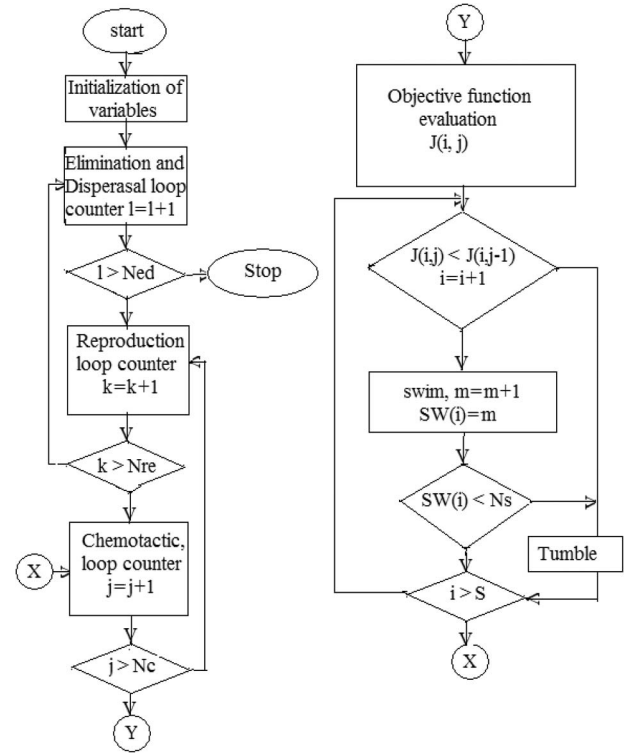


Fig. 1. Flowchart of the BF optimization algorithm.

- 4) The number of reproduction steps N_{re} is set to four.
- 5) The number of elimination and dispersal events N_{ed} is set to two.
- 6) The probability of elimination/dispersal p_{ed} is set to 0.25.
- 7) The location of each bacterium, which is a function of several parameters, i.e., $f(p_{ed}, N_b, N_c, N_{re}, N_{ed})$, is specified by a random number in the range [0–1].

Taking the guidance from the standard values available in the literature [18], we have experimented with a range of values on all kinds of images and noticed a considerable saving in computation time by reducing the number of iterations without losing the quality. The computation time varies according to the image size. For a normal image of size 1 megapixel, the bacteria can be as low as 12, and the number of chemotactic steps can be 25 or less, but a higher value like 50 is found to yield faster convergence of the solution. The parameters selected in this paper are applicable to the different images used for the enhancement.

G. Algorithm for Image Enhancement

- Step 1) Input the given image and convert RGB to HSV.
- Step 2) Calculate the histogram $p(x)$, where $x \in V$.
- Step 3) Calculate the initial value of f_h using (5).
- Step 4) Compute the values of exposure and a using (1) and (2), respectively.
- Step 5) Fuzzify V to get $\mu_{Xu}(x)$ and $\mu_{Xo}(x)$ using (4) and (6), respectively.
- Step 6) Initialize $\mu_c \leftarrow 0.5$, calculate C_{fus} , C_{fos} , C_{afus} , C_{afos} , Q_{fus} , and Q_{fos} , and initially set $t \leftarrow 0.5$ and $\gamma \leftarrow 2$.

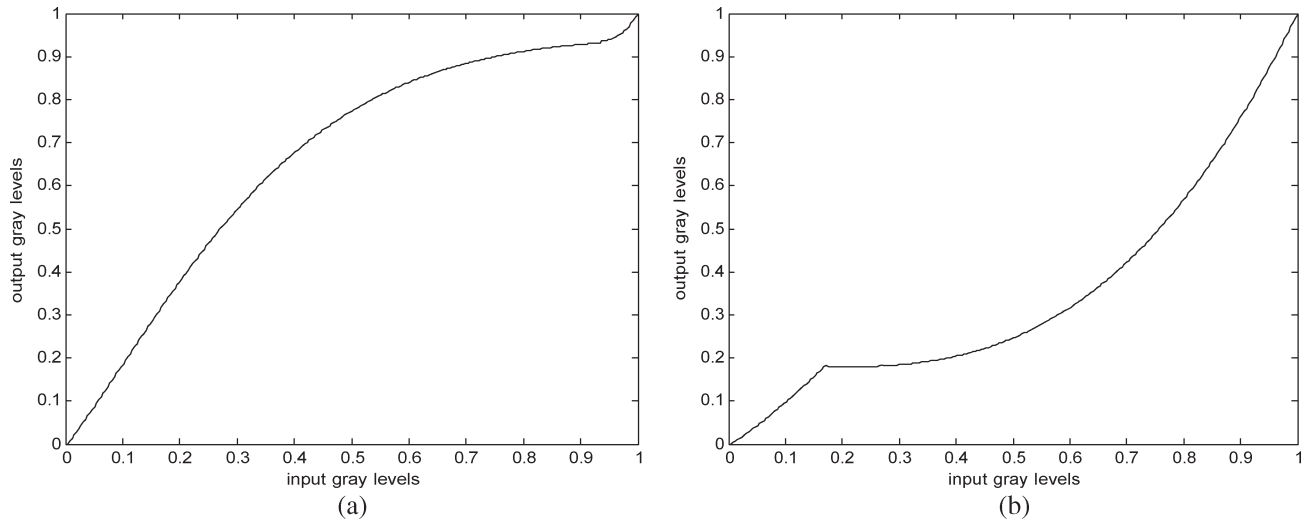


Fig. 2. (a) Transformation curve employed for the “Doctor” image. (b) Transformation curve employed for the “Man” image.

- Step 7) Calculate the modified membership values $\mu'_{Xu}(x)$ and $\mu'_{Xo}(x)$ for the underexposed region and the overexposed region using (7) and (8), respectively.
- Step 8) Now, calculate C_{fu} , C_{fo} , C_{afu} , C_{afo} , Q_{fu} , and Q_{fo} from the initial assumed values for parameters t , μ_c , f_h , and γ .
- Step 9) Calculate the visual factor V_f and set the desired visual factor $V_{df} \leftarrow 1.5$ to iteratively learn the parameters (t , μ_c , f_h , and γ).
- Step 10) Optimize the cost (i.e., objective) function using the modified BF algorithm and repeat step 7 to calculate the modified membership values for the optimized parameter set (t , μ_c , f_h , γ).
- Step 11) Defuzzify the modified membership values $\mu'_{Xu}(x)$ and $\mu'_{Xo}(x)$ using the inverse MFs

$$x'_u = \mu_{Xu}^{-1}[\mu'_{Xu}(x)] \quad (27)$$

$$x'_o = \mu_{Xo}^{-1}[\mu'_{Xo}(x)]. \quad (28)$$

Furthermore, combine them based on the value of a to obtain the enhanced intensity (V') as follows:

$$x' = \begin{cases} x'_u & \text{for } 0 \text{ to } a - 1 \\ x'_o & \text{for } a \text{ to } L - 1. \end{cases} \quad (29)$$

It may be noted from (29) that to obtain x' , x'_u will be needed for the gray levels (0 to $a - 1$), and x'_o will be needed for the gray levels (a to $L - 1$). Now, x' (modified gray levels) are mapped to x (original gray levels) to get the enhanced intensity V' .

- Step 12) Enhance the saturation for the overexposed images using (9) and display the enhanced HSV image.

V. RESULTS AND DISCUSSIONS

The proposed approach has been implemented using MATLAB. Around 50 images of both underexposed and overexposed types are considered as test images, and some of them are presented here.

For evaluating the performance of the proposed approach, the objective measures such as the visual factors and entropy



Fig. 3. (a) Original image. (b) Enhanced image of “Lena.”

are utilized. Generally, a direct application of the operators on the image indefinitely enhances, leading to the binarization of the image. To avoid this situation, the amount of enhancement is controlled by learning the parameters (t , μ_c , f_h , and γ) using the optimization of the objective function.

The sigmoid operator enhances the intensity, while the power law reduces the intensity; because of this, a discontinuity is observed at the intensity level a . This discontinuity causes unexpected blurring in the image. To get rid of this effect, the values of power-law operator are reduced while iteratively increasing the values of the sigmoid operator until both become equal at the intensity value a . Some nonlinear transformation curves of images such as the “Doctor” and “Man” images appear as in Fig. 2 after the application of the two operators. These curves are different for different images, depending on the nature of the images and the type of operators used.

For the subjective evaluation of the appearance, a few of the test images, namely, “Lena,” “Doctor,” “Face,” “Cricketer,” “Cougar,” and “Flower,” are shown in Figs. 3–8 and those of “Rose,” “Hills,” “Man,” and “Scene” are shown in Figs. 9–12. Figs. 9–12 contain both underexposed and overexposed regions, and in these figures, the original underexposed images have poor brightness, and the overexposed images have higher brightness. In both the cases, the details are not discernable, and the colors are not perceivable to the eyes.

It is noticed from experimentation that most of the underexposed images do not need enhancement of saturation. Coming to the overexposed image, it is desirable to observe the



Fig. 4. (a) Original image. (b) Enhanced image of “Doctor.”

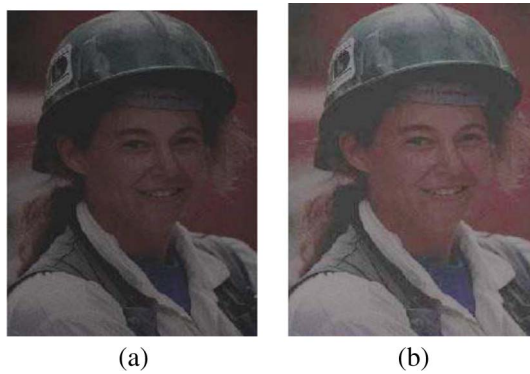


Fig. 5. (a) Original image. (b) Enhanced image of “Face.”

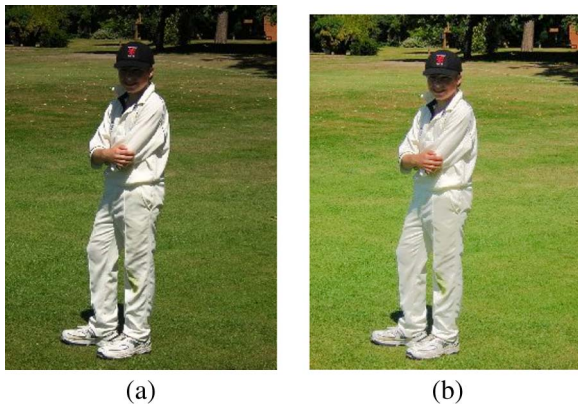


Fig. 6. (a) Original mixed-type image (“Cricketer”). (b) Enhanced image of “Cricketer.”



Fig. 7. (a) Original image (“Cougar”). (b) Enhanced image of “Cougar.”

permanently degraded regions in the images, namely, “Man” and “Rose,” to get a feel. The sole enhancement of intensity in this case is not sufficient to produce a good image, as the

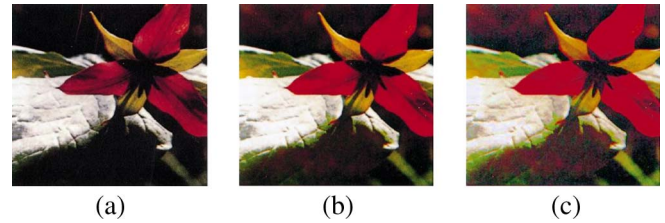


Fig. 8. (a) Original image. (b) Enhanced with GA-based approach [7]. (c) Enhanced image of “Flower” with the proposed approach.

intensity values of that region contain no information about the image. The information in these areas can be recovered up to some extent through the improvement or restoration of saturation using the saturation operator.

The proposed approach is compared with the existing GA-based approach [7] and entropy-based approach [13]. The procedure for calculating the visual factor for the entropy-based approach is discussed in Appendix B. For the subjective evaluation, Fig. 8 gives the comparison of the proposed approach with the GA-based approach, and Figs. 9–12 show the comparison of the proposed approach with entropy-based approach. It may be observed from these figures that the improvement attained with the proposed approach is more pleasing in nature than that with these two approaches, which overenhance certain regions as they do not consider underexposed and overexposed regions of the image while processing.

Table I represents the initial values of the parameters, entropy, and visual factors of the test images. It may be noted that the initial value of f_h is higher for the overexposed images. Table II represents the optimized parameters (the fuzzifier f_h , the crossover point, the intensifier t , and γ), visual factors, and entropy. The visual factor defined above can be used as a quantitative measure. Note that the visual factors V_{fu} and V_{fo} indicate the amount of enhancement done on the underexposed region and overexposed region, respectively. A value of one indicates that no enhancement or little enhancement is done. In Table II, a value of zero for V_{fo} for the images “Doctor” and “Lena” indicates that the power operator (8) is not applied on the image, as they do not have any overexposed region.

The objective assessment of visual appearance is shown in Table III. In Table III, it can be observed that the visual factors obtained with the proposed approach are more than those of the entropy-based approach [13]. It may be noted that the “Doctor” image has no overexposed region; hence, it is entirely enhanced as the underexposed image. The “Face” image has more improvement in the underexposed region than the amount of enhancement in the overexposed region. This fact cannot be ascertained from the visual appearance. However, “Rose” does indicate more improvement in the exposed region. In contrast to this, the visual factors of “Cougar” show more of enhancement and less of improvement. One can visually see that this is true. The overall visual factor is in between the visual factors of underexposed and overexposed regions. Thus, the proposed visual factors provide an idea that an improvement/enhancement has taken place in the appearance of the image, which is very difficult to visually judge at times.

As the proposed approach operates on the frequency of occurrence of gray levels rather than individual intensities of

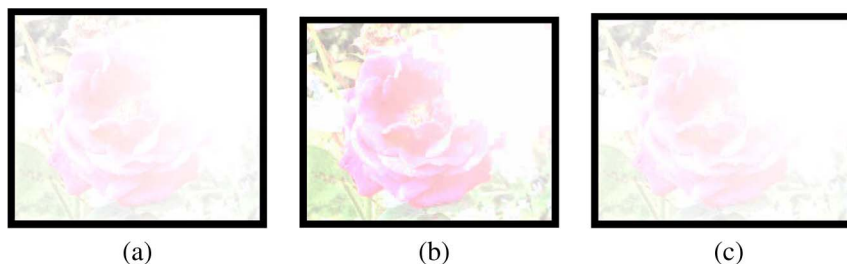


Fig. 9. (a) Original image of “Rose.” (b) Enhanced image of “Rose” with the proposed approach. (c) Modified image of “Rose” with the entropy-based approach.

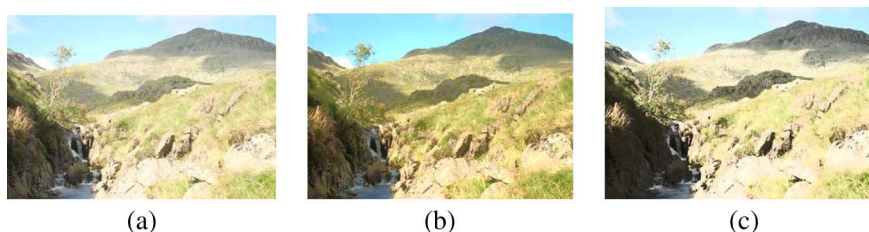


Fig. 10. (a) Original image (“Hills”). (b) Image of “Hills” with the proposed approach. (c) Modified image with the entropy-based approach.



Fig. 11. (a) Original image (“Man”). (b) Enhanced image with the proposed approach. (c) Modified image with the entropy-based approach.

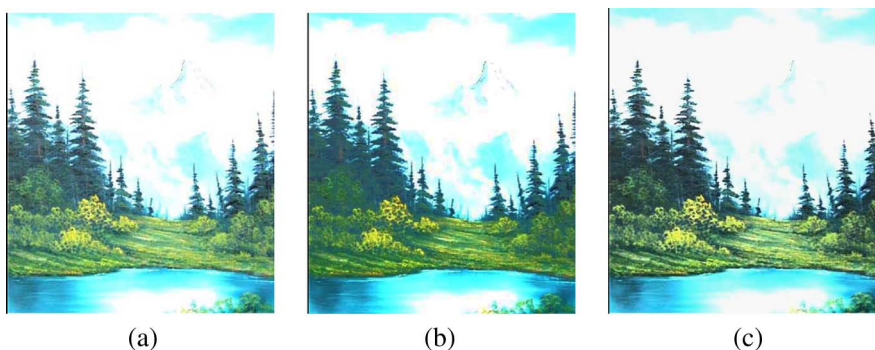


Fig. 12. (a) Original image (“Scene”). (b) Enhanced image with the proposed approach. (c) Modified image with the entropy-based approach.

pixels, this makes it computationally efficient. Fig. 13 shows the histogram for the image “Hills” before and after applying our approach. Note that the proposed approach reserves the histogram modes of the image.

VI. CONCLUSION

Fuzzy logic-based image enhancement has been undertaken by fuzzifying the color intensity property of an image. An image may be categorized into underexposed and overexposed regions with the amount of exposure indicated by a parameter. A

Gaussian MF suitable for underexposed region of the image has been used for the fuzzification. Enhancement of the fuzzified image has been carried out using a generalized intensification operator, i.e., GINT, of sigmoid type, which depends on the crossover point and the intensification parameter. A triangular MF has been used for the fuzzification of overexposed region of the image, and a power-law transformation operator has been used for the enhancement that depends on the gamma parameter. The optimum values of these parameters have been obtained by the constrained fuzzy optimization. BF involving an iterative learning has been adapted for the optimization. We

TABLE I
INITIAL VALUES OF PARAMETERS

Test Image	t	μ_c	f_h	γ	E	V_{fu}	V_{fo}	V_f
Hills	7.000	0.5000	113.4121	2.000	0.6592	0.8995	1.2891	1.1278
Man	7.000	0.5000	84.2980	2.000	0.5769	1.8543	1.3395	1.4843
Cricketer	7.000	0.5000	128.7328	2.000	0.5193	1.1561	1.1996	1.1655
Cougar	7.000	0.5000	155.5812	2.000	0.4705	1.1527	1.1583	1.1529
Doctor	7.000	0.5000	91.7695	2.000	0.4069	0.9630	0.0000	0.8990
Face	7.000	0.5000	137.1829	2.000	0.3949	1.7540	1.6441	1.7467
Scene	7.000	0.5000	100.3832	2.000	0.6385	1.3144	1.2049	1.2451
Rose	7.000	0.5000	179.8247	2.000	0.4969	0.9995	1.8558	1.5815
Flower	7.000	0.5000	159.3265	2.000	0.6034	0.9550	1.2520	1.0003
Lena	7.000	0.5000	69.0506	2.000	0.3436	1.4167	0.0000	1.3503

TABLE II
OPTIMIZATION OF $J = E + |V_{df} - V_f|$ WITH $V_{df} = 1.5$

Test Image	t	μ_c	f_h	γ	E	V_{fu}	V_{fo}	V_f
Hills	6.9985	0.5999	74.3919	2.3188	0.6614	1.4069	1.4258	1.4180
Man	3.3536	0.4177	82.7786	2.1645	0.4686	1.5466	1.5129	1.5224
Cricketer	6.5120	0.5756	92.6453	2.2963	0.4395	1.4273	1.2657	1.3926
Cougar	6.3778	0.5689	76.2770	2.2902	0.4070	1.4870	1.1690	1.4696
Doctor	7.0000	0.6000	79.7629	2.3188	0.2885	1.3644	0.0000	1.2738
Face	4.4025	0.4701	89.2218	2.2052	0.4248	1.5768	2.0765	1.6100
Scene	6.9955	0.5998	81.1621	2.3186	0.6418	1.7267	1.2752	1.4410
Rose	3.0049	0.4002	79.2678	2.1518	0.4713	1.0082	1.8802	1.6009
Flower	6.9981	0.5999	90.2467	2.3187	0.4609	1.3746	1.3684	1.3736
Lena	5.2845	0.5142	87.7552	2.2419	0.3342	1.6365	0.0000	1.5598

TABLE III
COMPARISON OF VISUAL FACTORS WITH THE
ENTROPY-BASED APPROACH

Images	V_f of Entropy [13] approach	V_f of proposed approach
Man	1.0894	1.5224
Scene	1.2264	1.4410
Rose	1.0277	1.6009
Hills	1.0780	1.4180

have also introduced entropy and visual factors as objective measures for evaluating the appearance of images.

A visually pleasing image has been obtained with the appropriate choice of contrast factors. It may be noted that GINT and power-law operators are controlled by these factors since ultimate enhancement leads to the binarization of the image. The results of the proposed enhancement approach using fuzzy entropy optimization have been compared with the recent GA-based approach [7] and entropy-based approach [13]. The parameter exposure determines the type of an image. For the case of permanently degraded images, the technique can re-

cover the lost details with saturation enhancement only up to some extent. For the complete recovery, replacement of information drawn from a similar texture patch is suggested in [17].

Several contributions made as part of this work include: 1) demarcation of an image into underexposed, overexposed, and mixed types; 2) presentation of separate operators for enhancement and objective measures for the assessment of the image quality achieved; and 3) modification of BF for improving its computational efficiency. As the work undertaken here is new, it should invigorate the readers for further exploration.

APPENDIX A BF FOR OPTIMIZATION

A new evolutionary computation technique, called the BF scheme, has recently been introduced [20]. Foraging can be modeled as an optimization process where bacteria seek to minimize the effort spent per unit time in foraging. In this scheme, an objective function is posed as the effort or a cost incurred by the bacteria in search of food. A set of bacteria tries to reach an optimum cost by following four stages such as chemotaxis, swarming, reproduction, and elimination and

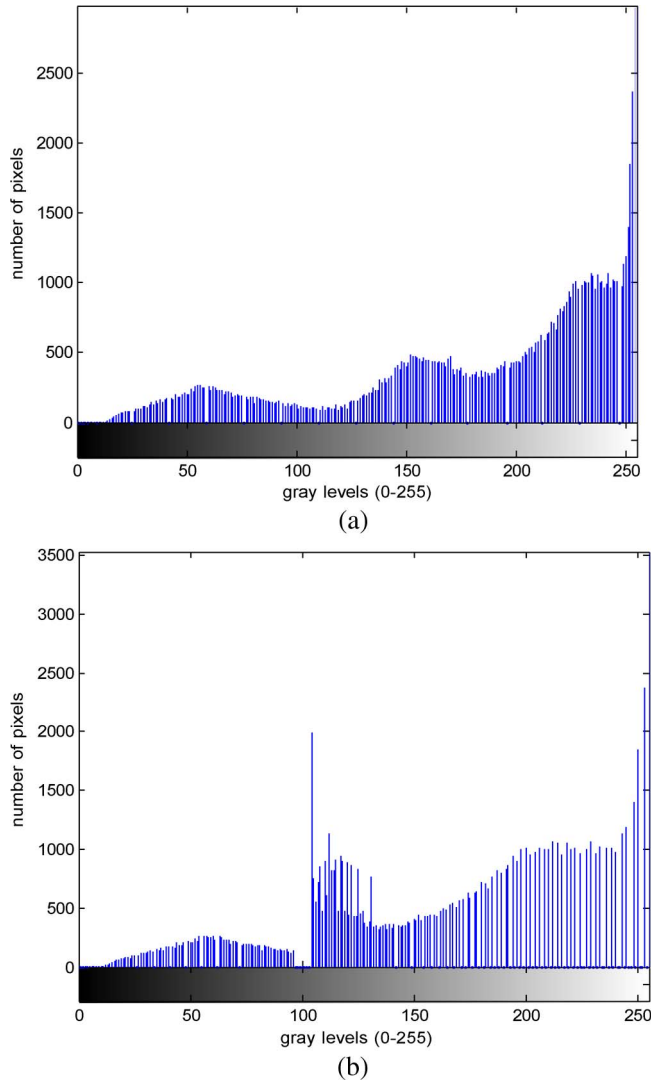


Fig. 13. Histogram for the image "Hills" (a) before and (b) after applying the proposed approach.

dispersal. There will be as many solutions as the number of bacteria. However, to arrive at an optimum path in the minimum time (i.e., convergence of solution path), we must have a sufficient number of bacteria. The bacteria have to follow four steps in the course of foraging.

In the chemotaxis stage, the bacteria either resort to a tumble followed by a run or make a tumble followed by a swim. On the other hand, in swarming, each *E. coli* bacterium signals another via attractants to swarm together. Furthermore, the least healthy bacteria die during the reproduction, whereas each of the healthiest bacteria splits into two, which are placed at the same location. While in the elimination and dispersal stage, any bacterium from the total set can be either eliminated or dispersed to a random location during the optimization. This stage helps the bacteria avoid the local optimum. Note that out of many bacteria engaged in foraging (several solution paths), some come out successful in achieving an optimum cost (an optimum solution). We will now introduce some parameters in J of (26), which allow its value to vary as the bacteria pass through various stages.

Let θ be the position of a bacterium and $J(\theta)$ in (26) as a function of θ represent the value of the objective function; then, the conditions $J(\theta) < 0$, $J(\theta) = 0$, and $J(\theta) > 0$ indicate whether the bacterium at location θ is in nutrient-rich, neutral, and noxious environments, respectively. Basically a chemotaxis is a foraging behavior that implements a type of optimization. Here, bacteria climb up the nutrient concentration (find the lower values of $J(\theta)$), avoid the noxious substances, and search for ways out of neutral media (avoid being at positions θ where $J(\theta) \geq 0$). The four basic iterative steps of BF optimization are now explained.

- 1) *Chemotaxis*: This step consists of a tumble followed by a tumble or a tumble followed by a run. Let j be the index of the chemotactic step, k be the index of the reproduction step, and l be the index of the elimination–dispersal event. Suppose that the position of each member in the population of bacteria N_b at the j th chemotactic step, k th reproduction step, and l th elimination–dispersal event be given by

$$P(j, k, l) = \{\theta^i(j, k, l) | i = 1, 2, \dots, N_b\}. \quad (\text{A.1})$$

Instead of $J(\theta)$, we consider $J(i, \theta^i(j, k, l))$ or simply $J(i, j, k, l)$ as the cost at the location of the i th bacterium $\theta^i(j, k, l) \in \mathcal{R}_p$ (a space of real values of P) and N_c to be the length of the lifetime of the bacteria as measured by the number of chemotactic steps. To represent a tumble, a unit length in the random direction, e.g., $\varphi(j)$, is generated. In particular, we take

$$\theta^i(j+1, k, l) = \theta^i(j, k, l) + D(i)\varphi(j) \quad (\text{A.2})$$

so that $D(i) > 0$, $i = 1, 2, \dots, N_b$, is the size of the step made in the random direction specified by the tumble. If at $\theta^i(j+1, k, l)$, the cost $J(i, j+1, k, l)$ is better (lower) than that at $\theta^i(j, k, l)$, then another step of size $D(i)$ will be made in the same direction. This movement, called swim, can be made in either direction in contrast to a tumble. It is continued until the cost is reduced but limiting the maximum number of steps N_s .

- 2) *Swarming*: As part of this task, the bacteria following the optimum path of food try to attract other bacteria so that together they more rapidly reach the desired location. The effect of swarming is to introduce an additional cost in $J(i, j, k, l)$. However, this step is ignored in the modified BF.
- 3) *Reproduction*: For reproduction, the population is sorted in the ascending order of accumulated food so that out of the total number of bacteria N_b , the least healthy bacteria N_{br} die and the healthiest bacteria N_{br} reproduce (split into two) with no mutations. Note that $N_{br} = N_b/2$, and let N_{re} be the number of reproduction steps.
- 4) *Elimination and dispersal*: This step helps reduce the behavior of *stagnation* (i.e., being trapped in a premature solution point or local optima). Each bacterium in the population undergoes this event with probability p_{ed} , and let N_{ed} be the number of these events.

APPENDIX B
CALCULATION OF VISUAL FACTOR FOR THE
ENTROPY-BASED APPROACH

As the fuzzy measures defined in Section IV are not directly applicable to the entropy-based approach [13], the following assumptions are made for the calculation of visual factors.

- 1) The crossover point is equal to 0.5.
- 2) $\mu_X(x)$ is S-MF, and $\mu'_X(x)$ is the INT operator as defined in [13].

The fuzzy contrast and average fuzzy contrasts for the original image and enhanced image can be calculated by

$$C_f = \frac{1}{L} \sum_{x=0}^{L-1} [\mu'_X(x) - \mu_c]^2 p(x) \quad (\text{B.1})$$

$$C_{af} = \frac{1}{L} \sum_{x=0}^{L-1} [\mu'_X(x) - \mu_c] p(x) \quad (\text{B.2})$$

$$C_{fo} = \frac{1}{L} \sum_{x=0}^{L-1} [\mu_X(x) - \mu_c]^2 p(x) \quad (\text{B.3})$$

$$C_{afo} = \frac{1}{L} \sum_{x=0}^{L-1} [\mu_X(x) - \mu_c] p(x). \quad (\text{B.4})$$

Next, the contrast factors and visual factors can be obtained from

$$Q_f = \frac{|C_{af}|}{C_f} \quad (\text{B.5})$$

$$Q_{fo} = \frac{|C_{afo}|}{C_{fo}} \quad (\text{B.6})$$

$$V_f = \frac{Q_f}{Q_{fo}}. \quad (\text{B.7})$$

REFERENCES

- [1] Z. Rahman, D. J. Jobson, and G. A. Woodell, "Multi-scale retinex for color image enhancement," in *Proc. IEEE Int. Conf. Image Process.*, 1996, vol. 3, pp. 1003–1006.
- [2] K. V. Velde, "Multi-scale color image enhancement," in *Proc. IEEE Int. Conf. Image Process.*, 1999, vol. 3, pp. 584–587.
- [3] L. Tao and V. Asari, "Modified luminance based MSR for fast and efficient image enhancement," in *Proc. IEEE 32nd AIPR*, 2003, pp. 174–179.
- [4] R. Eschbach and N. Y. Webster, "Image-dependent exposure enhancement," Patent number 5 414 538, May 9, 1995. U.S. patent [19].
- [5] R. Eschbach and B. W. Kolpatzik, "Image-dependent color saturation correction in a natural scene pictorial image," Patent number 5 450 217, Sep. 12, 1995. U.S. Patent [19].
- [6] S. K. Naik and C. A. Murthy, "Hue-preserving color image enhancement without gamut problem," *IEEE Trans. Image Process.*, vol. 12, no. 12, pp. 1591–1598, Dec. 2003.
- [7] M. Shyu and J. Leoua, "A genetic algorithm approach to color image enhancement," *Pattern Recognit.*, vol. 31, no. 7, pp. 871–880, Jul. 1998.
- [8] S. K. Pal and A. Rosenfeld, "Image enhancement and thresholding by optimization of fuzzy compactness," *Pattern Recognit. Lett.*, vol. 7, no. 2, pp. 77–86, Feb. 1988.
- [9] F. Russo and G. Ramponi, "A fuzzy operator for the enhancement of blurred and noisy images," *IEEE Trans. Image Process.*, vol. 4, no. 8, pp. 1169–1174, Aug. 1995.
- [10] P. Dong-Liang and X. An-Ke, "Degraded image enhancement with applications in robot vision," in *Proc. IEEE Int. Conf. Syst., Man, Cybern.*, Oct. 2005, vol. 2, pp. 1837–1842.
- [11] K. Arakawa, "Fuzzy rule based signal processing and its applications to image restoration," *IEEE J. Sel. Areas Commun.*, vol. 12, no. 9, pp. 1495–1502, Dec. 1994.
- [12] F. Russo, "Recent advances in fuzzy techniques for image enhancement," *IEEE Trans. Image Process.*, vol. 47, no. 6, pp. 1428–1434, Dec. 1998.
- [13] H. D. Cheng, Y.-H. Chen, and Y. Sun, "A novel fuzzy entropy approach to image enhancement and thresholding," *Signal Process.*, vol. 75, no. 3, pp. 277–301, Jun. 1999.
- [14] M. Hanmandlu, S. N. Tandon, and A. H. Mir, "A new fuzzy logic based image enhancement," *Biomed. Sci. Instrum.*, vol. 34, pp. 590–595, 1997.
- [15] H. Li and H. S. Yang, "Fast and reliable image enhancement using fuzzy relaxation technique," *IEEE Trans. Syst., Man, Cybern.*, vol. 19, no. 5, pp. 1276–1281, Sep./Oct. 1989.
- [16] M. Hanmandlu and D. Jha, "An optimal fuzzy system for color image enhancement," *IEEE Trans. Image Process.*, vol. 15, no. 10, pp. 2956–2966, Oct. 2006.
- [17] L. Wang, L. Wei, K. Zhou, B. Guo, and H. Shum, "High dynamic range image hallucination," in *Proc. Eurographics Symp. Rendering*, 2007.
- [18] R. C. Gonzalez and R. E. Woods, *Digital Image Processing*. Reading, MA: Addison-Wesley, 1992.
- [19] S. S. Rao, *Optimization: Theory and Application*, 2nd ed. New Delhi, India: New Age Int., 1995.
- [20] K. M. Passino, "Biomimicry of bacterial foraging for distributed optimization and control," *IEEE Control Syst. Mag.*, vol. 22, no. 3, pp. 52–67, Jun. 2002.



Madasu Hanmandlu (M'02–SM'06) received the B.E. degree in electrical engineering from Osmania University, Hyderabad, India, in 1973, the M.Tech. degree in power systems from Regional Engineering College Warangal, Jawaharlal Nehru Technological University, Hyderabad, in 1976, and the Ph.D. degree in control systems from the Indian Institute of Technology, New Delhi (IIT Delhi), India, in 1981.

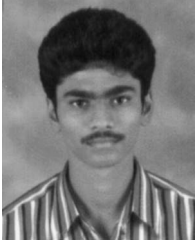
He is currently with Department of Electrical Engineering, IIT Delhi, where he was a Senior Scientific Officer with the Applied Systems Research Program (ASRP) from 1980 to 1982 and became a Lecturer in 1982, an Assistant Professor in 1990, an Associate Professor in 1995, and, finally, a Professor in 1997. He was with the Machine Vision Group, City University, London, from April to November 1988 and with the Robotics Research Group, Oxford University, Oxford, U.K., from March to June 1993, as part of the Indo–U.K. research collaboration. From March 2001 to March 2003, he was a Visiting Professor with the Faculty of Engineering, Multimedia University, Cyberjaya, Malaysia. He is the author of a book on computer graphics published in 2005 under PBP Publications. He is also the author of more than 185 publications in both conference proceedings and journals. He has guided 15 Ph.D. students and 82 M.Tech. students. He has handled several sponsored projects. He worked in the areas of power systems, control, robotics, and computer vision, before shifting to fuzzy theory. His current research interests mainly include fuzzy modeling for dynamic systems and applications of fuzzy logic to image processing, document processing, medical imaging, multimodal biometrics, surveillance, and intelligent control.

He is currently an Associate Editor for both *Pattern Recognition* journal and *IEEE TRANSACTIONS ON FUZZY SYSTEMS* and a Reviewer to *Pattern Recognition Letters*, *IEEE TRANSACTIONS ON IMAGE PROCESSING* and *IEEE TRANSACTIONS ON SYSTEMS, MAN, AND CYBERNETICS*. He is listed in *Reference Asia: Asia's Who's Who of Men and Women of Achievement* and *5000 Personalities of the World* (1998), published by the American Biographical Institute.



Om Prakash Verma received the B.E. degree in electronics and communication engineering from Malaviya National Institute of Technology, Jaipur, India, in 1991 and the M.Tech. degree in communication and radar engineering from the Indian Institute of Technology, New Delhi, India, in 1996. He is currently working toward the Ph.D. degree with the Department of Information Technology, Delhi College of Engineering.

From 1992 to 1998, he was a Lecturer with the Department of Electronics and Communication Engineering, Malaviya National Institute of Technology, Jaipur. In 1998, he joined the Department of Electronics and Communication Engineering, Delhi College of Engineering, New Delhi, India, as an Assistant Professor. He is currently the Head of the Department of Information Technology, Delhi College of Engineering. He is the author of a book on digital signal processing published in 2003. His research interests include image processing, application of fuzzy logic in image processing and digital signal processing.



Nukala Krishna Kumar received the B.Tech. degree in electronics and communications from the Nagarjuna Institute of Technology and Sciences Miryalguda, Jawaharlal Nehru Technological University, Hyderabad, India, in 2005 and the M.E. degree in electronics and communications from Delhi College of Engineering, New Delhi, India, in 2007.

He is currently a Software Engineer with Motorola India Pvt. Ltd., Hyderabad. His research interests include the application of fuzzy techniques to image processing problems.



Muralidhar Kulkarni received the B.E. degree in electronics engineering from University Visvesvaraya College of Engineering, Bangalore University, Bangalore, India, the M.Tech. degree in satellite communication and remote sensing from the Indian Institute of Technology, Kharagpur, India, and the Ph.D. degree in optical communication networks from Jamia Millia Islamia Central University, New Delhi, India.

From 1981 to 1982, he was a Scientist with the Instrumentation Division, Central Power Research Institute, Bangalore. From 1984 to 1988, he was an Aeronautical Engineer with the Avionics Group, Design and Development Team, Advanced Light Helicopter Project, Helicopter Design Bureau, Hindustan Aeronautics Ltd., Bangalore. From 1988 to 1994, he was a Lecturer of electronics engineering with the Electrical Engineering Department, University Visvesvaraya College of Engineering. From 1994 to 2008, he was an Assistant Professor with the Electronics and Communication Engineering Department, Delhi College of Engineering, New Delhi, where he has served as the Head of the Department of Information Technology and the Head of the Computer Center. He is currently a Professor with the Department of Electronics and Communication Engineering, National Institute of Technology Karnataka, Surathkal, India. He is the author of several research papers in national and international journals of repute. He is also the author of three very popular books in microwave and radar engineering, communication systems, and digital communications. His teaching and research interests are in the areas of digital communications, fuzzy digital image processing, optical communication and networks, and computer communication networks.